IBRO Neuroscience Reports 10 (2021) 31–41

Contents lists available at ScienceDirect

IBRO Neuroscience Reports

journal homepage: www.sciencedirect.com/journal/IBRO-Neuroscience-Reports

Research Paper

Deficits in pattern separation and dentate gyrus proliferation after rodent lateral fluid percussion injury

Erika A. Correll [a,1], Benjamin J. Ramser [b], Maxon V. Knott [c], Robert E. McCullumsmith [d,e], Jennifer L. McGuire [a], Laura B. Ngwenya [a,f,*]

[a] Department of Neurosurgery, University of Cincinnati, 231 Albert Sabin Way, Cincinnati, OH 45267, USA
[b] College of Medicine, University of Cincinnati, 231 Albert Sabin Way, Cincinnati, OH 45267, USA
[c] University of Cincinnati, 2600 Clifton Ave, Cincinnati, OH 45221, USA
[d] College of Medicine and Life Sciences, University of Toledo, 2801W. Bancroft St, Toledo, OH 43606, USA
[e] ProMedica Toledo Hospital, 1 ProMedica Pkwy, Toledo, OH 43606, USA
[f] Department of Neurology and Rehabilitation Medicine, University of Cincinnati, 231 Albert Sabin Way, Cincinnati, OH 45267, USA

ARTICLE INFO

Keywords:
Traumatic brain injury
Adult neurogenesis
Hippocampus

ABSTRACT

It has been demonstrated that adult born granule cells are generated after traumatic brain injury (TBI). There is evidence that these newly generated neurons are aberrant and are poised to contribute to poor cognitive function after TBI. Yet, there is also evidence that these newly generated neurons are important for cognitive recovery. Pattern separation is a cognitive task known to be dependent on the function of adult generated granule cells. Performance on this task and the relation to dentate gyrus dysfunction after TBI has not been previously studied. Here we subjected Sprague Dawley rats to lateral fluid percussion injury or sham and tested them on the dentate gyrus dependent task pattern separation. At 2 weeks after injury, we examined common markers of dentate gyrus function such as GSK3ß phosphorylation, Ki-67 immunohistochemistry, and generation of adult born granule cells. We found that injured animals have deficits in pattern separation. We additionally found a decrease in proliferative capacity at 2 weeks indicated by decreased phosphorylation of GSK3ß and Ki-67 immunopositivity as compared to sham animals. Lastly we found an increase in numbers of new neurons generated during the pattern separation task. These findings provide evidence that dentate gyrus dysfunction may be an important contributor to TBI pathology.

1. Introduction

Traumatic brain injury (TBI) effects over 2.8 million people in the US annually and over 69 million worldwide (Dewan et al., 2018; Taylor et al., 2017). Persons with TBI often suffer long-lasting cognitive deficits. The hippocampal dentate gyrus is an important brain region to investigate cognitive deficits after TBI, as the hippocampus is particularly vulnerable to injury, and increasing evidence suggests dentate gyrus dysfunction may be an important component of TBI pathology (Korgaonkar et al., 2020; Lowenstein et al., 1992; Toth et al., 1997). After experimental TBI there is an acute increase in production of new cells in the hippocampal dentate gyrus (Chirumamilla et al., 2002; Dash et al., 2001). Many of these new cells become adult generated neurons, however it is unclear how these new neurons contribute to cognitive recovery. It has been demonstrated that new neurons generated after TBI have abnormal features (Ibrahim et al., 2016; Ngwenya and Danzer, 2019; Ngwenya et al., 2018; Shapiro, 2017; Villasana et al., 2015), but also that they can have a functional role (Blaiss et al., 2011).

In uninjured brain, adult born neurons in the hippocampal dentate gyrus have been shown to be important for cognitive tasks. Specifically, pattern separation, the ability to distinguish two similar objects or spatial locations, has been shown to be dentate gyrus dependent and represent a functional role for adult neurogenesis (Bakker et al., 2008; Berron et al., 2016; Clelland et al., 2009). While there are well established cognitive behavioral deficits after experimental TBI, it has not been demonstrated whether a cognitive task known to be dentate gyrus dependent, such as pattern separation, is impaired. In this study, we use the rat lateral fluid percussion injury (LFPI) model to examine whether there are deficits in pattern separation, and whether there may be

* Correspondence to: Department of Neurosurgery, University of Cincinnati, 231 Albert Sabin Way, MSB 5251, Cincinnati, OH 45267, USA.
E-mail address: laura.ngwenya@uc.edu (L.B. Ngwenya).
[1] Present address: Neuroscience and Behavior Graduate Program, University of Massachusetts Amherst, 230 Stockbridge Road, Amherst, MA 01003, USA.

https://doi.org/10.1016/j.ibneur.2020.11.005
Received 15 May 2020; Accepted 27 November 2020

Nomenclature

IGCL	Inner granule cell layer
LFPI	Lateral fluid percussion injury
NOR	Novel object recognition
OGCL	Outer granule cell layer
RRT	Righting reflex time
TBI	Traumatic brain injury

evidence of dentate gyrus dysfunction that contributes to TBI pathology.

In addition to performance on the pattern separation task, we examined known influencers of adult neurogenesis and dentate gyrus function. We have previously shown that acutely after LFPI, there are changes in kinase activity with implications to proliferation and adult neurogenesis in the hippocampus (Dorsett et al., 2017). Specifically, GSK3ß is a key inhibitor of cell proliferation, modulates neuronal differentiation, and inhibition of GSK3ß has been considered as a therapeutic intervention for TBI (Hur and Zhou, 2010; Pardo et al., 2016; Shim and Stutzmann, 2016). Therefore, we examined GSK3ß expression given its known role in modulating proliferation. GSK3ß is constitutively active, and active GSK3ß halts proliferation and promotes maturation. When GSK3ß is phosphorylated, it is inactive, and no longer provides inhibition of proliferative pathways. A kinase that plays an important role in both upstream and downstream regulation of GSK3ß is AKT. We therefore explored whether there are differences in GSK3ß and AKT phosphorylation at 2 weeks after LFPI. Proliferation in the dentate gyrus granule cell layer increases after experimental TBI, so we investigated cell proliferation marker Ki-67 immunohistochemistry at 2 weeks after LFPI. Lastly, as adult born neurons are important for successful performance in pattern separation, we investigated whether new neurons were generated in LFPI animals in the same degree as in control animals by utilizing immunohistochemistry of the s-phase marker bromodeoxyuridine (BrdU) and immature neuronal marker doublecortin (DCX).

Here we show that 2 weeks after LFPI there are deficits in the dentate gyrus specific pattern separation task and alterations in proliferative capacity despite increased new neuron generation.

2. Material and methods

2.1. Animals

A total of 56 young adult male Sprague Dawley rats (8–9 weeks of age; weight 296.6 ± St. dev 18.2) obtained from Envigo (Indianapolis, IN) were used, with 39 included in this study. All animals were initially pair-housed in a 12 h light/dark cycle with access to food and water ad libitum. All animal care and experimental procedures were approved by the Institutional Animal Care and Use Committee and conformed to the National Institutes of Health Guide for the Care and Use of Laboratory Animals. After surgical procedures, animals were singly-housed in standard cages with enrichment. Animals were randomly assigned to sham or TBI groups and to tissue processing for immunoblotting (n = 8–10/group) or immunohistochemistry (n = 10–11/group).

2.2. Lateral fluid percussion injury

Anesthesia was induced via 4% isoflurane and maintained with 2–3% isoflurane throughout surgical procedures. All procedures followed sterile technique, including shaving the surgical site and sterilization with 70% alcohol and betadine solution. LFPI is a well-established model of experimental TBI (Thompson et al., 2005) and we performed the craniectomy surgery and lateral fluid percussion injury as previously described (McGuire et al., 2019; Sun et al., 2015; Van and Lyeth, 2016). Briefly, rats were mounted in a stereotaxic frame and a 4 mm diameter craniectomy was drilled with a trephine 4 mm posterior to bregma and 2.5 mm lateral of the sagittal suture, centered over the right parietal cortex. A plastic luer-loc hub was affixed over the craniectomy site with cyanoacrylate glue. A screw was inserted into the skull over the left parietal lobe which provided structural support for the dental acrylic cement that was applied to maintain the hub until injury. Animals that had violation of the dura during surgery were not continued in the study (11 animals). The incision was sutured shut and the plastic hub was covered with a screw-on cap. Animals were given one dose of 0.03 mg/kg sustained release Buprenorphine (0/7–1 mg/kg, ZooPharm) subcutaneously for post-op analgesia. Animals recovered from the procedure and lateral fluid percussion injury proceeded on day 3 after surgery. All animals received 5 min of anesthesia via inhalation of 4% isoflurane, the cap covering the craniectomy hub was removed and the hub was filled with saline to remove air bubbles and create a water tight seal to the output valve of the LFPI device. Animals in the injured group received a fluid pulse to the dura at a pressure of 2 atm (mean 2.2 ± 0.03) to induce a moderate injury. Sham animals were subjected to the same anesthetic and surgery protocols, but a fluid pulse was not delivered. After sham or injury, animals were laid on their back to assess time to spontaneously right (righting reflex time, RRT) as an index of injury severity. Injured animals that did not receive a fluid pulse of ~2 atm and/or had an inappropriate injury (RRT < 180 s; 1 animal) were excluded from further analysis. Five animals that received an appropriate injury, died as a result of the LFPI and were excluded from the study. After assessing RRT, animals were briefly re-anaesthetized via inhalation of 4% isoflurane, the surgical cement and hub were removed, and the surgical site was sutured closed with absorbable suture.

2.3. Bromodeoxyuridine administration

All animals received a single injection of 5'bromo-2'deoxyuridine (BrdU) on day 7 after LFPI to label proliferating cells. BrdU (Sigma B5002) was prepared in sterile saline at 10 mg/ml. A single 200 mg/kg dose of BrdU was injected intraperitoneally. Animals were perfused with 4% paraformaldehyde 8 days after administration (15 days after LFPI), as described below.

2.4. Behavioral testing

2.4.1. Habituation and baseline behavior

One week prior to surgical procedures animals were allowed to acclimate to the housing facility and underwent a habituation period that included handling, travel to the behavioral testing suite, administration of food treats (chocolate and fruit puffed cereal), and initiation of food restriction to encourage completion of behavioral tasks. For food restriction, animals were fed 5 g of food once-daily at completion of behavioral tasks, with daily weights to assure that animals did not lose ≥ 15% of their body weight. Baseline behavior included assessment of locomotor and anxiety behavior via 5 min exploration of a 50 gallon (63 cm diameter) open field arena (open field task). Animals were also habituated to the radial arm maze over a 3-day habituation period. On days one and two, animals were allowed free exploration of all eight food-baited arms for 15 min. On day three animals underwent a pre-injury working memory task, requiring visiting 7 of 8 un-baited arms in under 10 min with fewer than 4 arm revisits. All behavioral testing was video recorded and assessed using Ethovision XT 11.5 software (Noldus). Animals that could not complete this baseline task were excluded from the study. Animals that successfully completed the baseline behavior proceeded to surgical procedures. Two days post-injury, all animals were re-habituated to the radial arm maze in which they were allowed to explore the apparatus for 10 min without any treats present. Post-injury behavioral testing began 3 days post-injury (Fig. 1A). All animals underwent the full behavioral testing paradigm.

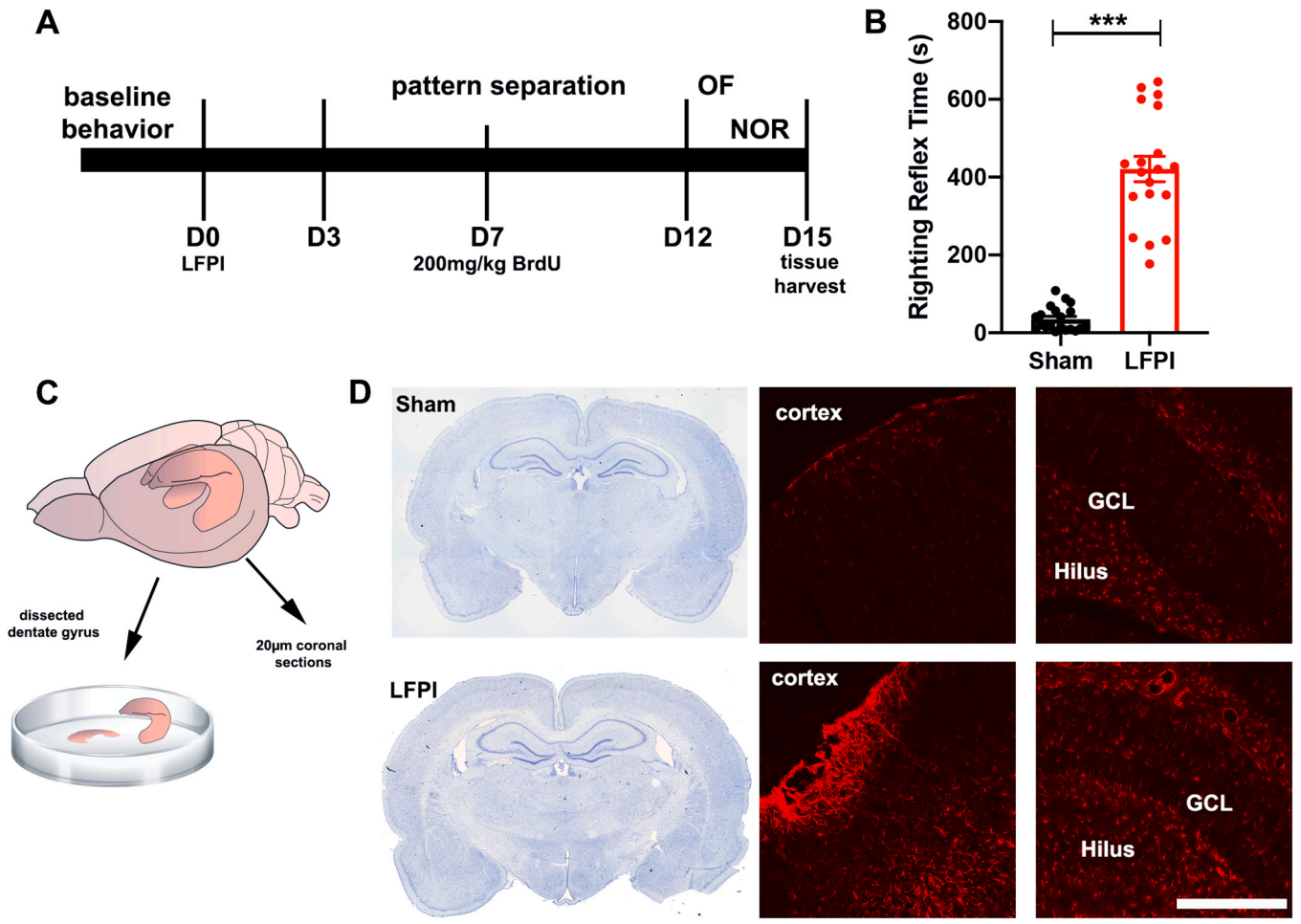

Fig. 1. (A) Experimental design. Animals received baseline behavior prior to LFPI on Day 0 (D0). Three days after LFPI (D3) pattern separation task was started and continued daily for 10 days through D12. On D7 animals received a single intraperitoneal injection of bromodeoxyuridine (BrdU) after completion of behavioral testing. On D13 animals were tested on open field arena (OF) and then on novel object recognition (NOR). Tissue was harvested at the completion of behavioral testing. (B) Animals that received LFPI had significantly longer righting reflex time (RRT) as compared to sham animals. Error bars are standard error of the mean; ***$p < 0.001$. (C) In animals for immunoblotting, the hippocampus was isolated from fresh tissue and the dentate gyrus was dissected. Animals for immunohistochemistry were perfused with 4% paraformaldehyde and were cryosectioned at 20 μm. (D) Representative stained sections are shown from Sham (top row) and LFPI (bottom row) animals processed 2 weeks after injury. Cresyl violet staining illustrates lack of gross cortical or hippocampal damage. However, injury is evidenced by increased glial activity seen with GFAP staining in cortex and hippocampal dentate gyrus. Scale bar for GFAP is 250 μm.

2.4.2. Pattern separation task

The pattern separation paradigm was designed as a delayed non-match to place task in the radial arm maze, similar to that presented by others (Clelland et al., 2009; Morris et al., 2012). Each testing trial was comprised of two phases: a "sample" phase in which all maze arms were closed except for the starting arm and the baited "sample" arm positioned 90 degrees relative to the starting position, and a "condition" phase where the baited arm was a new arm either separate or adjacent to the sample arm. The separate condition consisted of all arms of the maze being closed except for the starting arm, the sample arm, and the arm located directly across from the sample arm, giving a 3-arm degree of separation. In the adjacent condition all arms were closed except for the starting arm, the sample arm, and an adjacent arm with 0-arm degree of separation (Fig. 2A). Rats were given 90 s between the sample and condition phase, and 90 s during each phase to retrieve the treat from the baited arm.

A correct trial was scored when an animal entered the baited arm within 90 s. Animals that traveled to an incorrect arm were not allowed to self-correct and were removed from the maze immediately. A trial was coded as incomplete if the animal did not enter any arms in 90 s. All animals received a total of ten trials per day for ten consecutive days. Each trial condition was randomly predetermined to be a separate or adjacent condition and additionally the sample and condition arms were randomized. To minimize olfactory cues, the maze was cleaned with 70% ethanol in between each phase of the trial, in between trials, and in between testing of each animal. Pattern separation data was not used from animals that did not complete $\geq$ 75% of trials (6 Sham and 7 LFPI animals). All trials were video recorded with Ethovision software.

2.4.3. Open field activity task

To assess locomotor, hyperactivity, and anxiety behavior after injury, rats were allowed to explore the open arena. Distance traveled (in cm), velocity (cm/s), and time spent exploring the center of the arena (in seconds) were video recorded over a 5 min period by the Ethovision Software and confirmed by manual review of the video. The center of the arena was defined as the inner half (32 cm diameter). Each animal's performance in the open field as compared to their baseline was assessed for statistical differences between groups.

2.4.4. Novel object recognition

To test short term memory, rats were tested on a novel object recognition task within the open field arena. Animals were allowed to explore the arena for 10 min without any objects to re-familiarize them to the arena. The following day, the animals were placed in the arena for

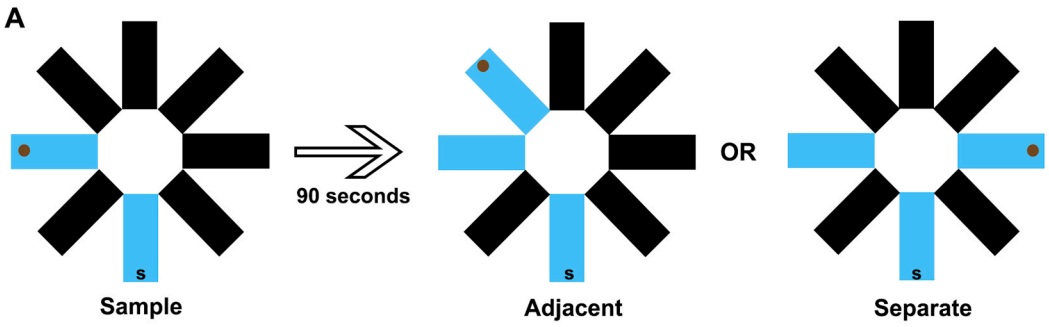

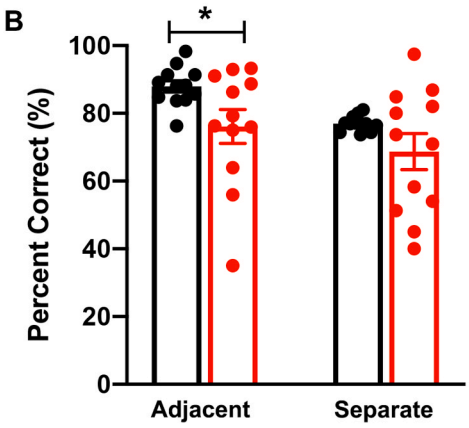

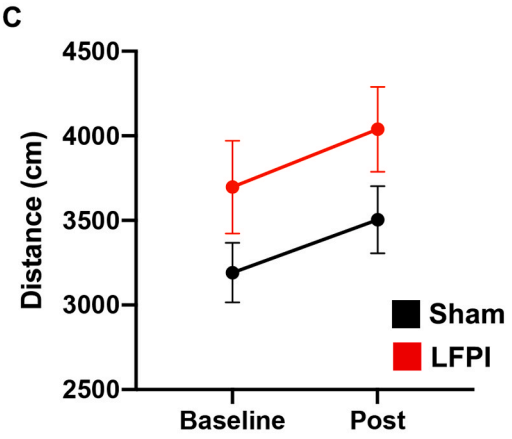

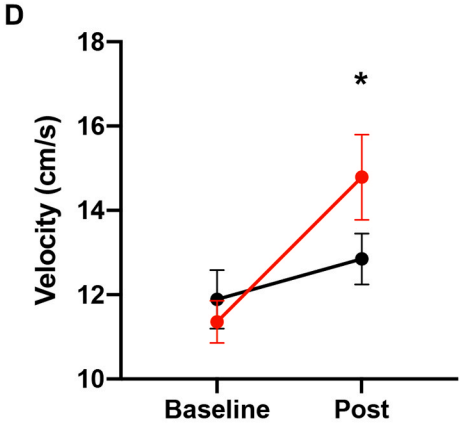

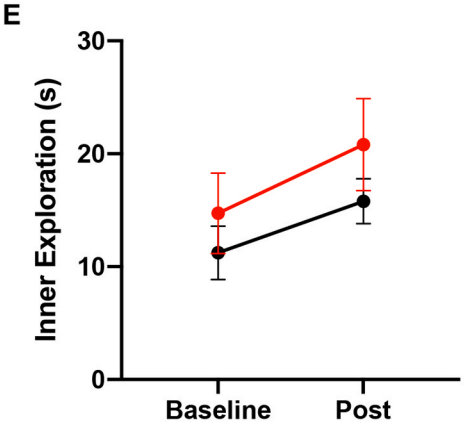

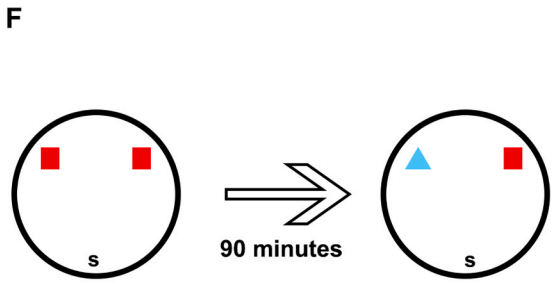

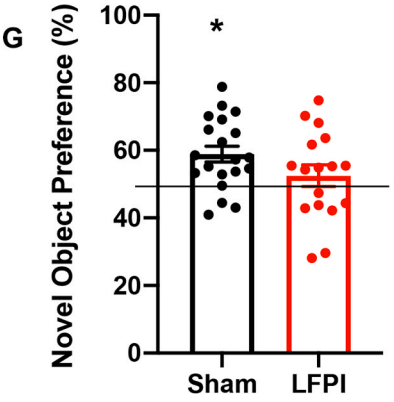

(caption on next page)

Fig. 2. (A) The pattern separation task consisted of a sample task where rats were placed in the start arm (s) and allowed to retrieve a treat from the open arm. After 90 s animals were tested on either an adjacent trial, where the arm next to the sample arm was baited with a treat, or a separate condition where the arm 180 degrees from the sample arm was baited. (B) Sham (black, n = 12) and LFPI (red, n = 12) animals performed similarly on the separate task, however LFPI animals (n = 12) performed worse than sham (n = 13) on the adjacent condition of the pattern separation task. (C) As compared to their baseline performance, there was no group difference between sham (n = 19) and LFPI animals (n = 16) in distance traveled in the open arena, however the LFPI animals traveled at a faster velocity (D). There was no significant group difference in time spent exploring the inner portion of the arena (E). (F) The novel object recognition task involved animals being allowed to explore the open arena with two identical objects. After 90 min they were placed in the arena with a familiar object, and a novel object. Time exploring the novel object relative to total time exploring was calculated as the discrimination ratio. (G) A novel object preference index of 50% (horizontal line) represents equal exploration of both objects. Sham animals (n = 20) performed statistically better than 50%, however LFPI animals (n = 17) did not. All error bars represent standard error of the mean; *p < 0.05. (For interpretation of the references to color in this figure legend, the reader is referred to the web version of this article.)

10 min with two identical objects affixed to opposite sides of the arena. After a 90 min interval, each rat was presented with one familiar object and one novel object and allowed to explore for 5 min. Preference Index was defined as a percentage representing time spent exploring the novel object ÷ total exploration time (x100). Preference Index > 50% was hence used to indicate novel object preference. Time exploring was calculated by manual review of the recorded videos. Exploration time was counted only when the animal was facing the object and interacting with the object (grooming near the object or backside towards the object were not counted as exploration). Data was not used from animals that had < 30 s of total exploration time or from trials where an object became dislodged from its position (2 LFPI animals). Objects and the side of novel object placement were alternated. Between novel and familiar trials and between each animal, all objects and the arena were cleaned with 70% ethanol to minimize olfactory cues.

2.5. Tissue acquisition

For immunohistochemical processing, rats were administered 1 ml/kg of anesthetic (ketamine 100 mg/ml, xylazine 10 mg/ml) prior to perfusion fixation. Animals were transcardially perfused with phosphate buffer followed by 4% paraformaldehyde, brains were post-fixed in 4% paraformaldehyde overnight at 4 °C and then submerged in graded sucrose solutions for cryoprotection. Brains were then flash frozen in cold isopentane and stored at − 80 °C until use. Brains were sectioned in the coronal plane on a cryostat at 20 μM thickness through the entirety of the hippocampus (Fig. 1B). Tissue was cut in six series and collected free-floating into vials of cryoprotectant and stored at − 20 °C until batch processed for immunohistochemistry.

For immunoblotting, rats were sacrificed via rapid decapitation using a guillotine. Brains were quickly removed and dissected in cold phosphate buffer (Fig. 1B). The brains were hemisectioned along the sagittal suture, thalamus and brainstem were removed, and the ipsilateral dentate gyrus was rapidly isolated with aid of a 27G needle tip and a dissecting microscope (Au - Hagihara et al., 2009). The tissue was immediately snap frozen on dry ice, and stored at − 80 °C until homogenized for protein analysis.

2.6. Immunoblotting

Dissected ipsilateral dentate gyrus samples were homogenized in 300 μL of Mammalian Protein Extraction Reagent (#78501 Thermo Scientific, Rockford, IL, USA) and 3 μL of HALT (#78440 Thermo Scientific). Samples were diluted to one half, one fourth, one tenth, and one twentieth and loaded in triplicates onto a 96 well plate. Two hundred microliters of working solution composed of 50-parts BCA reagent A (#23228 Thermo Scientific) to 1-part BCA reagent B (#23224 Thermo Scientific) was loaded into each well. The plate incubated at room temperature for 2 h. The final protein concentration for each sample was calculated from the absorbance measurements in μg/μL.

10 μg of protein in 10 μL sodium dodecyl sulfate sample buffer (#J61337 Alfa Aesar, Ward Hill, MA, USA) were loaded into a 15-well 4–15% Mini-PROTEAN TGX pre-cast gel (#4561086 Bio-Rad, Hercules, CA, USA) and ran at 200 V for 30 min in 1X Tris/Glycine/SDS Buffer made from 10x stock(#161-0732 Bio-Rad). The gel was then transferred onto an Immobilon-FL polyvinylidene transfer membrane (#IPFL00010 Merck Millipore Ltd., Burlington, MA, USA) at 20 V for 20 min via semi-dry transfer in 1X Tris/Glycine Buffer. Membranes were incubated in REVERT Total Protein Stain (#926-11010 Li-Cor Lincoln, NE, USA), washed and imaged using Li-Cor Odyssey imager for later signal normalization to total protein. After incubation in destaining solution (#926-11013 Li-Cor, Lincoln, NE, USA), membranes were blocked for 1 h in Odyssey Blocking Buffer (#927-50000 Li-Cor, Lincoln, NE, USA) at room temperature. Membranes were then incubated overnight at 4 °C in primary antibodies against the following proteins: mouse anti-total AKT (1:1000; #2920 Cell Signaling Technology, Danvers, MA), mouse anti-GSK3β (1:1000; #9832 Cell Signaling Technology), rabbit anti-pAKT S473, (#4058T Cell Signaling Technology, Danvers, MA, USA, 1:1000) or rabbit anti-pGSK-3β S9 (1:1000; #9336 Cell Signaling Technology). Total and phospho proteins were processed on the same blot. Membranes were washed is a tris-buffered saline with Tween-20 (TBS-T) incubated for 1 h at room temperature in fluorescent secondary antibodies: IRDye 800CW Donkey anti-mouse (1:20,000; #926-32212 Li-Cor,) IRDye 800CW Donkey anti-rabbit (1:20,000; #926-32213 Li-Cor), or IRDye 680RD Donkey anti-mouse (1:20,000; #925-68072 Li-Cor). Membranes were imaged on a Li-Cor Odyssey Imager.

Protein expression was normalized to total protein stain (Aldridge et al., 2008; Eaton et al., 2013; Kirshner and Gibbs, 2018). Results are presented as ratio of normalized phosphoprotein to normalized total protein for GSK3ß and AKT.

2.7. Histology and immunohistochemistry

2.7.1. Histological representation of injury

Tissue sections were processed for histological assessment of LFPI. Sham and LFPI animals were processed for cresyl violet. Slide mounting sections were briefly washed then submerged in 0.1% Cresyl Echt Violet (ScyTek Lab #CEA999). Slides were then rinsed in distilled water, followed by subsequent dehydration in graded ethanol solutions and cleared in xylene. Slides were coverslipped using permount.

Select sham and LFPI animals were processed for glial fibrillary acidic protein (GFAP) immunohistochemistry to characterize gliosis. Free-floating sections were washed in phosphate buffer and blocked in normal goat serum (NGS) for 30 min at room temperature. Following blocking, sections were incubated overnight at 4 °C in rabbit anti-GFAP antibody (1:500; DAKO ZO334) solution containing NGS and 0.3% Triton-x. Following primary antibody incubation, sections were washed then incubated in goat anti-rabbit IgG Alexa Fluor 568 secondary antibody (1:250; Invitrogen #A-11011) in the dark for 2 h at room temperature. Sections were then washed in buffer, mounted, and coverslipped with polyvinyl alcohol mounting medium with DABCO (Sigma).

2.7.2. Immunohistochemistry and stereological analysis of Ki-67

Tissue was batch processed to minimize procedural variance. Ki-67 immunohistochemistry was performed on every 24th section, spaced at 480 μM, throughout the entirety of the hippocampus. After removing the sections from − 20 °C and washing in phosphate buffer, an antigen retrieval step of tri-sodium citrate (pH 6) at 60 °C for 30 min was performed. After washing, sections were then blocked with 3% normal

horse serum (NHS) and 0.1% triton-x for 30 min at room temperature. Tissue was then incubated overnight at 4 °C in primary antibody solution consisting of mouse anti-Ki-67 (NCL-L-Ki67-MM1 Leica; 1:250), 3% NHS, and 0.1% triton-x. The following day, sections were washed and placed in biotinylated secondary antibody for 1 h at room temperature (biotinylated horse anti-mouse, BA-2000 Vector Labs, Burlingame, CA; 1:250; in 3% NHS with 0.1% triton-x). Tissue was quenched with cold 10% H_2O_2 in methanol prior to incubation in avidin-biotin complex (PK-6100 Vector Labs) and development with diaminobenzidine (SK-4100 Vector Labs). Sections were then mounted onto glass slides, counterstained with Cresyl Violet, and coverslipped.

The estimated total number of Ki-67+ cells was obtained for the granule cell layer by an operator blind to subject group. Ki-67 labeled nuclei were identified using a 100x oil objective on a Zeiss Axio Imager M2 (Carl Zeiss Microscopy GmbH; Jena, Germany), equipped with a motorized stage, and controlled by StereoInvestigator software (MicroBrightField; Williston, VT, USA). As Ki-67 labeling is rare, an optical fractionator with an exhaustive counting scheme (grid size equal to counting frame size) and guard planes was used, and estimates of total number of Ki-67+ cells were calculated using N = Q x 1/asf x 1/ssf x 1/tsf, as previously described (Ngwenya et al., 2005).

2.7.3. Fluorescence immunohistochemistry and analysis of BrdU and DCX

BrdU and DCX double fluorescence immunohistochemistry was performed on every 24th section, spaced at 480 μM, throughout the entirety of the hippocampus on a cohort of 12 animals. After removing the sections from − 20 °C and washing in phosphate buffer, sections were blocked for 30 min in 10% normal goat serum with 0.3% Triton-X then incubated in rabbit anti-DCX primary antibody (1:500; Cell Signaling 4604S) overnight at 4 °C. Sections were then washed and incubated in goat anti-rabbit Alexa Fluor 488 secondary antibody (1:250; #A-11034 Invitrogen) for 2 h at room temperature. Sections were then washed, fixed in 4% paraformaldehyde for 10 min at room temperature, incubated for 30 min in 2 N HCl at 37 °C, and blocked for 30 min prior to incubation overnight at 4 °C in primary antibody for BrdU (mouse anti-BrdU Roche 11170376001; 1:200). Sections were washed, incubated in goat anti-mouse Alexa Fluor 568 (1:250; #A-11004 Invitrogen) for 2 h at room temperature, and finally washed, mounted and coverslipped.

The estimated total number of BrdU+ cells in the granule cell layer was obtained by an operator blind to subject group. BrdU labeled nuclei were identified using a 100x oil objective on a Zeiss Axio Imager M2 (Carl Zeiss Microscopy GmbH; Jena, Germany), equipped with a motorized stage, and controlled by StereoInvestigator software (MicroBrightField; Williston, VT, USA). As BrdU labeling is rare, an optical fractionator with an exhaustive counting scheme including guard planes was used, as above. Tissue throughout the rostral-caudal extent of the hippocampus was analyzed for BrdU+ cells that were also positive for immature neuronal marker DCX. Double immunopositivity was confirmed using a 60x oil objective and 1 μm slice photographs through the z-axis. The ratio of double labeled/total BrdU+ cells examined was multiplied by the total BrdU+ cell population to obtain the estimated total number of BrdU+DCX+ cells per animal.

2.8. Statistical analysis

Statistical analysis was conducted using GraphPad Prism 8.0 for Windows (GraphPad Software). Normality of data was tested using the Shapiro-Wilk test. Statistical outliers were identified and excluded using ROUT method with Q = 1%. Open field data for each animal was compared to their baseline, thus a repeated measures ANOVA was performed. For all other data, differences between groups were analyzed via independent T-tests with Tukey post-hoc for analysis of multiple comparisons. NOR data was additionally calculated as a one-sample *t*-test against a chance value of 50%. For non-normally distributed data, group differences were determined with Mann–Whitney U. Significance was indicated by $p < 0.05$.

3. Results

3.1. Lateral fluid percussion produces reproducible consistent injuries

Sham injury was performed in 20 animals and LFPI in 19 animals. Sham animals had a mean RRT of 35.25 s (± std error of mean 7.0), whereas injured animals received a 2.17 atm injury (± 0.03) with a mean RRT of 420.8 s (± 32.8). There was a significant difference in RRT between sham and injured groups (Mann–Whitney U, $p < 0.0001$; Fig. 1B). As is typical in the LFPI model, large cortical cavitation was not seen, however injured animals showed increased staining with GFAP in the cortex at the injury site and the underlying hippocampal dentate gyrus (Fig. 1D).

3.2. Injured animals exhibit cognitive behavioral deficits

Fourteen Sham and twelve LFPI animals successfully completed the pattern separation task. Three sham animals had data points that were statistical outliers and removed from further analysis. Sham and LFPI animals performed similarly on the separate condition of the pattern separation task (sham mean 76.41 ± 0.87, LFPI mean 68.7 ± 5.34; $t(22) = 1.42$, $p = 0.168$; Fig. 2B). On the adjacent condition LFPI animals performed worse (sham mean 87.87 ± 1.5, LFPI mean 76.14 ± 5.02), with a statistically significant difference between groups ($t(23) = 2.31$, $p = 0.030$; Fig. 2B).

On the open field arena task, animals were tested on locomotor activity and compared to their baseline performance. There was no significant effect of time by injury group for distance traveled ($F(1,33) = 0.004$, $p = 0.95$; Fig. 2C). LFPI animals showed an increase in velocity after injury, with a significant effect of time by injury ($F(1,33) = 4.70$, $p = 0.038$; Fig. 2D).

Animals were tested for anxiety behavior by analysis of the amount of time spent exploring the center of the open arena. Sham and LFPI animals spent a similar amount of time exploring the center of the arena and there was no statistically significant effect of time by group ($F(1,33) = 0.078$, $p = 0.78$; Fig. 2E).

Short term memory was assessed by performance on the novel object recognition task. Equal time spent with the familiar and novel object after the 90 min interval (Fig. 2F) was defined as a novel object preference index of 50% (chance). Although Sham and LFPI animals did not have group means that were statistically different ($t(35) = 1.65$, $p = 0.109$), Sham animals performed statistically better than chance ($t(19) = 3.79$, $p = 0.0012$), whereas LFPI animals did not ($t(16) = 0.78$, $p = 0.448$; Fig. 2G).

3.3. GSK3β and AKT protein expression in dentate gyrus 2 weeks after LFPI

At 2 weeks after injury, LFPI animals showed a statistically significant decrease in phospho/total GSK3ß protein expression as compared to sham animals ($t(13) = 2.31$, $p = 0.038$; one statistical outlier per group; Fig. 3B). Yet, the ratio of phospho/total AKT protein expression was not statistically significant between groups ($t(14) = 1.43$, $p = 0.18$; one sham statistical outlier; Fig. 3D).

3.4. Proliferative capacity decreased 2 weeks after LFPI

Proliferative capacity in the dentate gyrus was examined by analysis of Ki-67+ nuclei in the granule cell layer of the dentate gyrus. The estimated total number of Ki-67 nuclei in the granule cell layer was decreased in the LFPI group 2 weeks after injury (2932 ± 244.7) as compared to sham animals (4366 ± 570.2), this was a statistically significant difference between groups ($t(19) = 2.39$, $p = 0.028$; Fig. 4C).

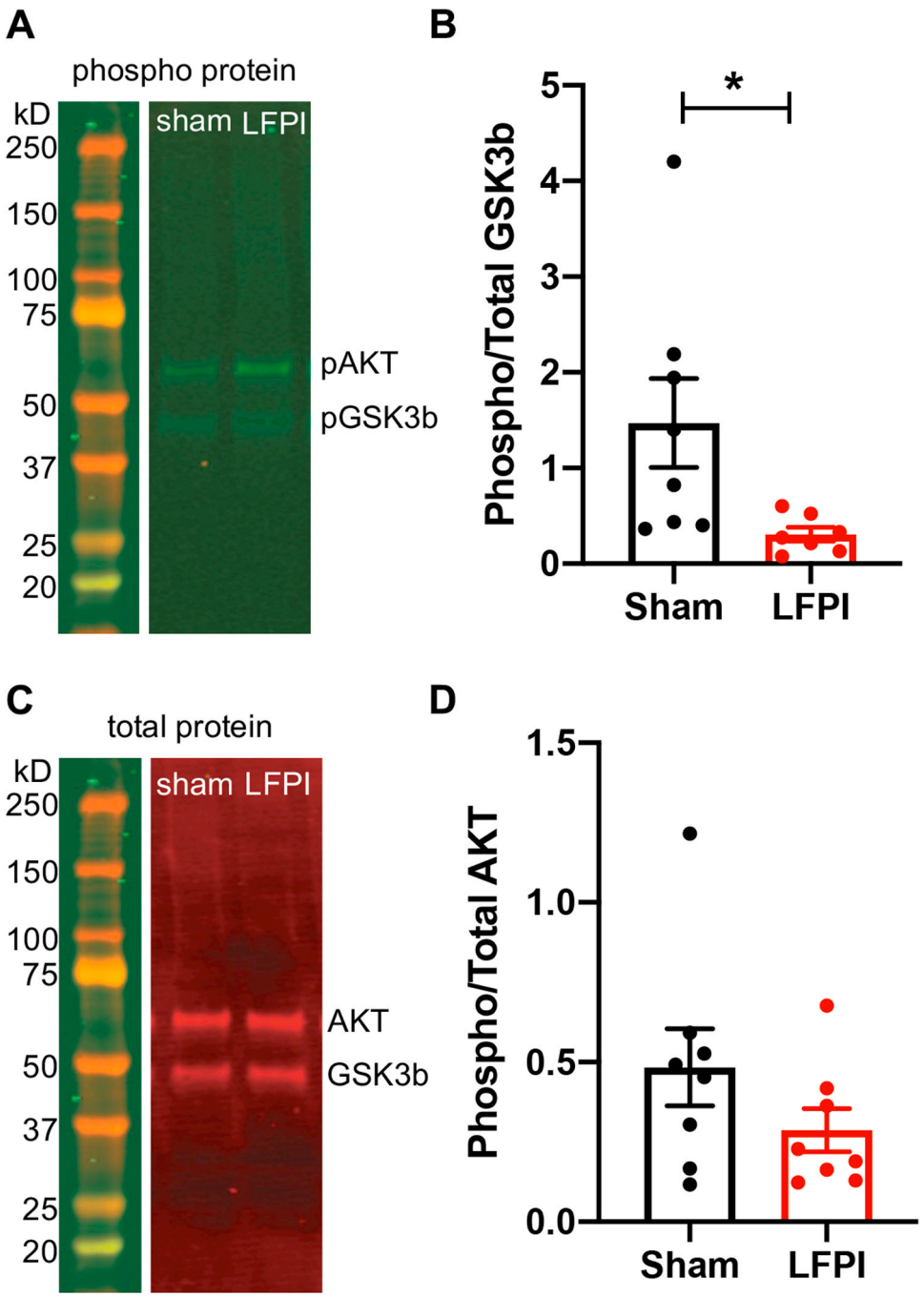

Fig. 3. (A) Representative immunoblots of phospho-AKT (pAKT) and phospho-GSK3ß (pGSK3). (B) The ratio of phospho/total GSK3ß protein expression was significantly decreased in LFPI animals (n = 7) compared to sham (n = 8). (C) Representative immunoblots of total AKT and total GSK3ß. (D) The phospho/total AKT did not show significant group differences in protein expression (n = 8/group). Error bars represent standard error of the mean; *p < 0.05.

3.5. Increased number of new neurons born during pattern separation

BrdU was administered at Day 7 after LFPI (midway through the 10-day pattern separation task) and tissue examined at Day 15 after LFPI. LFPI animals had a significantly larger total number of BrdU+DCX+ cells in the dentate gyrus (1727 ± 329.4, versus Sham mean 833.1 ± 73.2, p = 0.004; Fig. 4D).

4. Discussion

In summary, we have shown that LFPI animals have deficits in pattern separation, alterations in dentate gyrus GSK3ß protein expression, and increased numbers of adult born immature neurons despite decreased proliferative capacity at 2-weeks after injury.

Our data are consistent with others that show cognitive behavioral deficits after LFPI. In our model, we saw an increase in velocity after TBI, but no change in distance traveled, nor a decrease in time spent in the center of the open arena (suggesting no change in anxiety). Studies demonstrating anxiety after experimental TBI have used a diffuse and/or a severe TBI model and have also observed an anxious phenotype at chronic time points (1–6 months) after TBI (Heldt et al., 2014; Jones et al., 2008). Our model is a lateral, moderate injury, and we tested behavior at 2 weeks; this may explain the absence of a clear anxiety phenotype in our animals. We demonstrated deficits in novel object

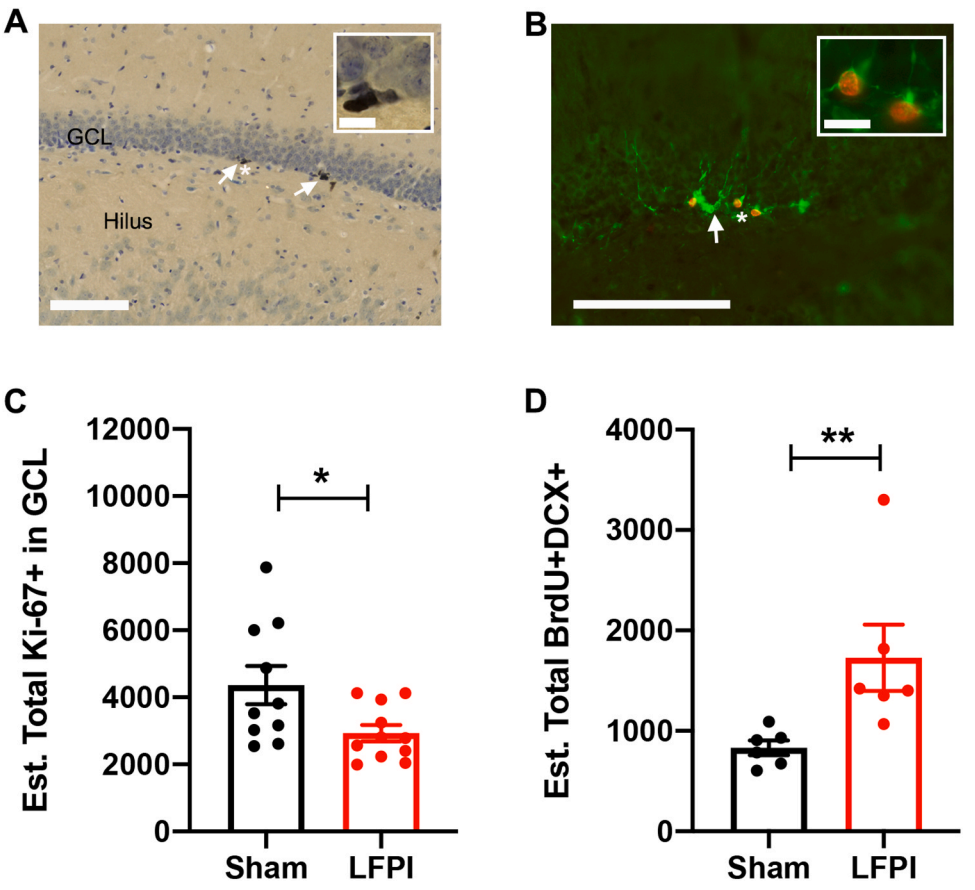

Fig. 4. (A) Representative photomicrograph of Ki-67 immunohistochemistry showing diaminobenzidine positive Ki-67+ nuclei (arrows) in the granule cell layer (GCL) with cresyl violet counterstain. Inset shows details of labeled nuclei at the asterisk. (B) Representative photomicrograph of bromodeoxyuridine (BrdU) and doublecortin (DCX) immunofluorescence. BrdU (red) and DCX (green) labeled cells were identified at the inner portion of the granule cell layer (arrow). Inset shows larger magnification of double labeled BrdU+DCX+ cells at the asterisk. Scale bars in A, B are 100 μm, inset scale bars 10 μm. (C) The total number of Ki-67+ cells in the dentate gyrus granule cell layer was decreased in the LFPI group (n = 11) compared to sham (n = 10) at 2 weeks. (D) Eight days after BrdU injection (15 days after LFPI), the total number of double labeled BrdU+DCX+ was increased in LFPI animals as compared to sham animals (n = 6/group). All error bars represent standard error of the mean; *p < 0.05, **p < 0.01.

recognition in LFPI animals, as our LFPI animals did not perform consistently better than chance (50%). However, there was significant individual variability in our animals which prohibited showing concrete differences between our Sham and LFPI groups. Short-term memory deficits in tasks such as NOR have been presented by others using varying experimental TBI models (Aungst et al., 2014; Hylin et al., 2013; Osier et al., 2015). NOR is thought to rely on the hippocampus, however other cortical regions likely play a role (Antunes and Biala, 2012), and additionally NOR is not specifically dependent on the dentate gyrus.

We are the first to demonstrate deficits in the dentate gyrus specific task, pattern separation, after experimental TBI. Pattern separation, the ability to discriminate highly similar context, has been attributed to the hippocampal dentate gyrus. Rodent dentate gyrus lesions (Gilbert et al., 2001; Morris et al., 2012) and receptor knockout studies (McHugh et al., 2007) as well as human functional MRI (Bakker et al., 2008; Berron et al., 2016) have localized pattern separation to the dentate gyrus and specifically to adult generated neurons (Clelland et al., 2009; Nakashiba et al., 2012; Sahay et al., 2011). Our LFPI model shows pattern separation deficits similar to what others have demonstrated with bilateral dentate gyrus selective lesions, namely preserved performance on the dissimilar (separate) condition of the task and deficits on the similar (adjacent) conditions. This suggests that although LFPI creates a heterogenous injury that likely involves multiple cortical, subcortical, and white matter pathways, the hippocampal dentate gyrus, and particularly the process of adult neurogenesis, may be especially vulnerable.

At 2 weeks after LFPI we found decreased phosphorylation of GSK3ß compared to sham animals, which could represent decreased proliferative capacity as pGSK3ß promotes proliferation. Akt is an important kinase both in upstream and downstream pathways for GSK3ß, yet surprisingly we did not find significant differences in AKT expression. This suggests that modulation of GSK3ß after LFPI may happen in an AKT independent manner. Although it should be noted that there was individual variability in our immunoblotting results which could have obscured our ability to find a significant difference in pAKT expression. Many experimental TBI models have shown increases in pGSK3ß, which seems contrary to our findings of decreased pGSK3ß. Others have reported acute changes in AKT and GSK3ß after experimental TBI. For example, Shapira et al. (2007) found increases in hippocampal pGSK3ß 24 h after a mild weight drop injury. Dash et al. (2011) found transient increases in pGSK3ß in hippocampal tissue at 24 h after CCI. Zhao et al. (2012) had similar findings in CCI cortical tissue, with increases in pGSK3ß at 24 and 72 h after injury, but no changes at their longest examined timepoint of 7 days after injury. They also found post-TBI increases in pAkt at 4 h after injury, similar to acute pAKT increases seen by others (Noshita et al., 2002). Limited studies have examined changes in pAkt and pGSK3ß expression at longer timepoints after experimental TBI. In a blast model of TBI, Wang et al. (2017) demonstrated increases in hippocampal pAkt and pGSK3ß sustained at 6 weeks after injury. In a CCI model, Wu et al. (2013) showed increases in cortical pGSK3ß expression that peaked at 3 days after injury, remained elevated at 14d, and returned to control levels at 28 days. Although these findings appear contradictory to our results, there are many study variables which could explain the different findings. We used a LFPI model and examined hippocampal dentate gyrus tissue specifically, not cortex or whole hippocampi. No other study to date has specifically examined dentate gyrus GSK3ß expression at 2 weeks after LFPI. In addition, all of our animals received cognitive testing, yet the direct impact of the testing and the implications of our decreased pGSK3ß findings relative to cognition is limited, as we harvested tissue for immunoblotting the day after completion of all cognitive testing. As this timepoint is not *immediately* after behavior testing, and kinase changes can be acute and short lasting, our findings may not accurately reflect kinase activity in relation to cognitive testing. The decreased pGSK3ß results may instead represent the "baseline" kinase activity in the sham

and LFPI animals, and thus direct correlations to cognitive behavior are limited. However, in a mouse knockin model of GSK3ß (replicates decreased pGSK3ß as the knockin GSK3ß cannot be phosphorylated and thus GSK3ß is hyperactive), GSK3ß knockin animals had worse performance on NOR and decreased hippocampal dentate gyrus proliferation (Pardo et al., 2016). Our results, although different than what some others have published in experimental TBI, are consistent in reflecting the purported role of GSK3ß in both cognition and proliferation.

Decreased proliferative capacity after LFPI is further supported by our Ki-67 results. We see a statistically significant decrease in the estimated total number of Ki-67+ cells in the dentate gyrus at 2 weeks after injury. These findings can have a number of interpretations: that well-documented early increases in proliferation after TBI (Chirumamilla et al., 2002; Dash et al., 2001) are diminished by 2 weeks, that the enrichment of behavioral testing enhances proliferation in sham animals to a different degree than injured animals, or perhaps that the population of active stem cells becomes depleted (Encinas and Sierra, 2012; Neuberger et al., 2017). The proliferative capacity at extended timepoints after TBI has not been thoroughly studied. Some have found a return to baseline proliferation at 2 to 3 weeks after injury using different animal models or analysis techniques than presented here (Rola et al., 2006; Sun et al., 2005). For instance, Sun et al. (2005) showed acute increases in proliferation as measured by BrdU injection 24 h before sacrifice. They found increases in proliferation at 2 and 7 days, but a return to baseline (not a decrease) at 14 days after LFPI. BrdU labels cells in the S-phase of the cell cycle, whereas Ki-67 labels all non-resting cells, these differences in methodology may explain the differences in results. Interestingly, Gaulke et al. (2005) provided environmental enrichment to rats after LFPI and at 3 weeks after injury found no difference in Ki-67+ cells between sham, injured, and injured enriched groups, however they note a trend towards a decreased number of Ki-67+ cells in the injured enriched group despite better performance on the Morris Water Maze task. In rat LFPI, Neuberger et al. (2017) demonstrated large increases in proliferation at 3 to 7 days post injury with a statistically significant decline in neurogenic potential 3 months later. Similarly, in a rat CCI model, Acosta et al. (2013a, 2013b) have demonstrated significant decreases in Ki-67+ cells at 8 weeks after injury. The interplay between enrichment, behavioral testing paradigms, and neurogenic potential after TBI deserves further research to determine the implications of our findings and the relevance to cognitive performance.

We additionally showed an increase in numbers of adult born granule cells after LFPI. BrdU was administered 7 days after LFPI. Our increase in total BrdU+DCX+ cells suggests that many of the newly generated cells at 7 days after LFPI adopt a neuronal phenotype by 2 weeks after injury. Despite an increase in immature neurons, LFPI animals showed deficits in the pattern separation task that is new neuron dependent. Although this suggests that the newly generated neurons are improperly integrated or dysfunctional, there are some considerations and limitations to the interpretation of our findings. The age and maturity of when new neurons best contribute to cognitive testing is unclear. Our experimental paradigm labeled cells being generated at day four of the 10-day pattern separation task. It is unclear if these early neurons would have opportunity to contribute to the cognitive tasks being performed. Additionally, these data represent a snapshot of the new neurons generated at day seven after LFPI, but we cannot assume from our data that this increase in new neuron generation is equivalent at day one or day 10 after injury.

Although we show deficits in cognitive tasks in the setting of increased new neuron generation, others have shown that the integration of new neurons is crucial to cognitive recovery. Sun et al. (2015) have shown that abolishing new neuron generation after LFPI in rats does not affect performance on the Morris Water Maze task at 21–24 days post-TBI, however TBI animals show innate recovery in this task when tested at 56–60 days after injury and early abolishment of adult born neurons impairs this recovery. Blaiss et al. (2011) have also shown, in a murine controlled cortical impact model of TBI, that elimination of injury-induced neurogenesis impairs performance and recovery on the Morris Water Maze task. Hence, performance on the pattern separation task at longer time points after experimental TBI and determination of the role of newly generated neurons in successful completion of this task after injury are indicated.

4.1. Conclusion

This is the first study to show deficits in the dentate gyrus specific task, pattern separation, after experimental TBI. Our combined findings of impaired performance in pattern separation, decreased proliferative capacity, and increased adult born neuron generation deserves further study to better understand how adult neurogenesis after injury influences cognitive performance. Our findings provide supporting evidence that dentate gyrus dysfunction may be an important component of TBI pathology.

Funding

This research was supported by a University of Cincinnati Gardner Neurosciences Institute Neurobiology Research Center Pilot Grant (LBN) and by NIH/NINDS K08NS110988 (LBN).

Compliance with Ethical Standards

The authors certify that all experiments were carried out in accordance with the National Institute of Health Guide for the Care and Use of Laboratory Animals. Formal approval to conduct the experiments described has been obtained from the University of Cincinnati Institutional Animal Care and Use Committee review board. Documentation of approved animal procedures can be provided upon request.

CRediT authorship contribution statement

Erika A. Correll: Methodology, Investigation, Writing - original draft. **Benjamin J. Ramser**: Investigation, Writing - original draft. **Maxon V. Knott**: Investigation, Validation, Formal analysis. **Robert E. McCullumsmith**: Conceptualization, Supervision. **Jennifer L. McGuire**: Conceptualization, Supervision, Writing - original draft, Formal analysis. **Laura B. Ngwenya**: Conceptualization, Formal analysis, Visualization, Writing - review & editing, Supervision, Funding acquisition.

Acknowledgements

The authors wish to thank Judy Bohnert, Alexandra Lowery, and Tracy Hopkins, MS for technical assistance, and Inkosi Media, LLC for assistance with figure design. We would also like to acknowledge the Live Imaging Core at the University of Cincinnati.

Conflicts of Interest

The authors have no competing interests to declare.

References

Acosta, S.A., Diamond, D.M., Wolfe, S., Tajiri, N., Shinozuka, K., Ishikawa, H., Hernandez, D.G., Sanberg, P.R., Kaneko, Y., Borlongan, C.V., 2013a. Influence of post-traumatic stress disorder on neuroinflammation and cell proliferation in a rat model of traumatic brain injury. PLoS One 8, e81585. https://doi.org/10.1371/journal.pone.0081585.

Acosta, S.A., Tajiri, N., Shinozuka, K., Ishikawa, H., Grimmig, B., Diamond, D., Sanberg, P.R., Bickford, P.C., Kaneko, Y., Borlongan, C.V., 2013b. Long-term upregulation of inflammation and suppression of cell proliferation in the brain of adult rats exposed to traumatic brain injury using the controlled cortical impact model. PLoS One 8, e53376. https://doi.org/10.1371/journal.pone.0053376.

Aldridge, G.M., Podrebarac, D.M., Greenough, W.T., Weiler, I.J., 2008. The use of total protein stains as loading controls: an alternative to high-abundance single-protein controls in semi-quantitative immunoblotting. J. Neurosci. Methods 172, 250–254. https://doi.org/10.1016/j.jneumeth.2008.05.003.

Antunes, M., Biala, G., 2012. The novel object recognition memory: neurobiology, test procedure, and its modifications. Cogn. Process. 13, 93–110. https://doi.org/10.1007/s10339-011-0430-z.

Au - Hagihara, H., Au - Toyama, K., Au - Yamasaki, N., Au - Miyakawa, T., 2009. Dissection of hippocampal dentate gyrus from adult mouse. J. Vis. Exp., e1543 doi: 10.3791/1543.

Aungst, S.L., Kabadi, S.V., Thompson, S.M., Stoica, B.A., Faden, A.I., 2014. Repeated mild traumatic brain injury causes chronic neuroinflammation, changes in hippocampal synaptic plasticity, and associated cognitive deficits. J. Cereb. Blood Flow Metab. Off. J. Int. Soc. Cereb. Blood Flow Metab. 34, 1223–1232. https://doi.org/10.1038/jcbfm.2014.75.

Bakker, A., Kirwan, C.B., Miller, M., Stark, C.E., 2008. Pattern separation in the human hippocampal CA3 and dentate gyrus. Science 319, 1640–1642. https://doi.org/10.1126/science.1152882.

Berron, D., Schutze, H., Maass, A., Cardenas-Blanco, A., Kuijf, H.J., Kumaran, D., Duzel, E., 2016. Strong evidence for pattern separation in human dentate gyrus. J. Neurosci. Off. J. Soc. Neurosci. 36, 7569–7579. https://doi.org/10.1523/JNEUROSCI.0518-16.2016.

Blaiss, C.A., Yu, T.S., Zhang, G., Chen, J., Dimchev, G., Parada, L.F., Powell, C.M., Kernie, S.G., 2011. Temporally specified genetic ablation of neurogenesis impairs cognitive recovery after traumatic brain injury. J. Neurosci. Off. J. Soc. Neurosci. 31, 4906–4916. https://doi.org/10.1523/JNEUROSCI.5265-10.2011.

Chirumamilla, S., Sun, D., Bullock, M.R., Colello, R.J., 2002. Traumatic brain injury induced cell proliferation in the adult mammalian central nervous system. J. Neurotrauma 19, 693–703. https://doi.org/10.1089/08977150260139084.

Clelland, C.D., Choi, M., Romberg, C., Clemenson, G.D., Fragniere, A., Tyers, P., Jessberger, S., Saksida, L.M., Barker, R.A., Gage, F.H., Bussey, T.J., 2009. A functional role for adult hippocampal neurogenesis in spatial pattern separation. Science 325, 210–213. https://doi.org/10.1126/science.1173215.

Dash, P.K., Johnson, D., Clark, J., Orsi, S.A., Zhang, M., Zhao, J., Grill, R.J., Moore, A.N., Pati, S., 2011. Involvement of the glycogen synthase kinase-3 signaling pathway in TBI pathology and neurocognitive outcome. PLoS One 6, e24648. https://doi.org/10.1371/journal.pone.0024648.

Dash, P.K., Mach, S.A., Moore, A.N., 2001. Enhanced neurogenesis in the rodent hippocampus following traumatic brain injury. J. Neurosci. Res. 63, 313–319 doi: 10.1002/1097-4547(20010215)63:4<313::AID-JNR1025>3.0.CO;2-4.

Dewan, M.C., Rattani, A., Gupta, S., Baticulon, R.E., Hung, Y.C., Punchak, M., Agrawal, A., Adeleye, A.O., Shrime, M.G., Rubiano, A.M., Rosenfeld, J.V., Park, K.B., 2019. Estimating the global incidence of traumatic brain injury. J. Neurosurg. 130, 1080–1097. https://doi.org/10.3171/2017.10.JNS17352.

Dorsett, C.R., McGuire, J.L., Niedzielko, T.L., DePasquale, E.A., Meller, J., Floyd, C.L., McCullumsmith, R.E., 2017. Traumatic brain injury induces alterations in cortical glutamate uptake without a reduction in glutamate transporter-1 protein expression. J. Neurotrauma 34, 220–234. https://doi.org/10.1089/neu.2015.4372.

Eaton, S.L., Roche, S.L., Llavero Hurtado, M., Oldknow, K.J., Farquharson, C., Gillingwater, T.H., Wishart, T.M., 2013. Total protein analysis as a reliable loading control for quantitative fluorescent Western blotting. PLoS One 8, e72457. https://doi.org/10.1371/journal.pone.0072457.

Encinas, J.M., Sierra, A., 2012. Neural stem cell deforestation as the main force driving the age-related decline in adult hippocampal neurogenesis. Behav. Brain Res. 227, 433–439. https://doi.org/10.1016/j.bbr.2011.10.010.

Gaulke, L.J., Horner, P.J., Fink, A.J., McNamara, C.L., Hicks, R.R., 2005. Environmental enrichment increases progenitor cell survival in the dentate gyrus following lateral fluid percussion injury. Brain Res. Mol. Brain Res. 141, 138–150. https://doi.org/10.1016/j.molbrainres.2005.08.011.

Gilbert, P.E., Kesner, R.P., Lee, I., 2001. Dissociating hippocampal subregions: double dissociation between dentate gyrus and CA1. Hippocampus 11, 626–636. https://doi.org/10.1002/hipo.1077.

Heldt, S.A., Elberger, A.J., Deng, Y., Guley, N.H., Del Mar, N., Rogers, J., Choi, G.W., Ferrell, J., Rex, T.S., Honig, M.G., Reiner, A., 2014. A novel closed-head model of mild traumatic brain injury caused by primary overpressure blast to the cranium produces sustained emotional deficits in mice. Front. Neurol. 5, 2. https://doi.org/10.3389/fneur.2014.00002.

Hur, E.M., Zhou, F.Q., 2010. GSK3 signalling in neural development. Nat. Rev. Neurosci. 11, 539–551. https://doi.org/10.1038/nrn2870.

Hylin, M.J., Orsi, S.A., Zhao, J., Bockhorst, K., Perez, A., Moore, A.N., Dash, P.K., 2013. Behavioral and histopathological alterations resulting from mild fluid percussion injury. J. Neurotrauma 30, 702–715. https://doi.org/10.1089/neu.2012.2630.

Ibrahim, S., Hu, W., Wang, X., Gao, X., He, C., Chen, J., 2016. Traumatic brain injury causes aberrant migration of adult-born neurons in the hippocampus. Sci. Rep. 6, 21793. https://doi.org/10.1038/srep21793.

Jones, N.C., Cardamone, L., Williams, J.P., Salzberg, M.R., Myers, D., O'Brien, T.J., 2008. Experimental traumatic brain injury induces a pervasive hyperanxious phenotype in rats. J. Neurotrauma 25, 1367–1374. https://doi.org/10.1089/neu.2008.0641.

Kirshner, Z.Z., Gibbs, R.B., 2018. Use of the REVERT((R)) total protein stain as a loading control demonstrates significant benefits over the use of housekeeping proteins when analyzing brain homogenates by Western blot: an analysis of samples representing different gonadal hormone states. Mol. Cell. Endocrinol. 473, 156–165. https://doi.org/10.1016/j.mce.2018.01.015.

Korgaonkar, A.A., Nguyen, S., Li, Y., Sekhar, D., Subramanian, D., Guevarra, J., Pang, K. C.H., Santhakumar, V., 2020. Distinct cellular mediators drive the Janus faces of toll-like receptor 4 regulation of network excitability which impacts working memory performance after brain injury. Brain Behav. Immun. 88, 381–395. https://doi.org/10.1016/j.bbi.2020.03.035.

Lowenstein, D.H., Thomas, M.J., Smith, D.H., McIntosh, T.K., 1992. Selective vulnerability of dentate hilar neurons following traumatic brain injury: a potential mechanistic link between head trauma and disorders of the hippocampus. J. Neurosci. Off. J. Soc. Neurosci. 12, 4846–4853.

McGuire, J.L., Correll, E.A., Lowery, A.C., Rhame, K., Anwar, F.N., McCullumsmith, R.E., Ngwenya, L.B., 2019. Pioglitazone improves working memory performance when administered in chronic TBI. Neurobiol. Dis. 132, 104611 https://doi.org/10.1016/j.nbd.2019.104611.

McHugh, T.J., Jones, M.W., Quinn, J.J., Balthasar, N., Coppari, R., Elmquist, J.K., Lowell, B.B., Fanselow, M.S., Wilson, M.A., Tonegawa, S., 2007. Dentate gyrus NMDA receptors mediate rapid pattern separation in the hippocampal network. Science 317, 94–99. https://doi.org/10.1126/science.1140263.

Morris, A.M., Churchwell, J.C., Kesner, R.P., Gilbert, P.E., 2012. Selective lesions of the dentate gyrus produce disruptions in place learning for adjacent spatial locations. Neurobiol. Learn. Mem. 97, 326–331. https://doi.org/10.1016/j.nlm.2012.02.005.

Nakashiba, T., Cushman, J.D., Pelkey, K.A., Renaudineau, S., Buhl, D.L., McHugh, T.J., Barrera, V.R., Chittajallu, R., Iwamoto, K.S., McBain, C.J., Fanselow, M.S., Tonegawa, S., 2012. Young dentate granule cells mediate pattern separation, whereas old granule cells facilitate pattern completion. Cell 149, 188–201. https://doi.org/10.1016/j.cell.2012.01.046.

Neuberger, E.J., Swietek, B., Corrubia, L., Prasanna, A., Santhakumar, V., 2017. Enhanced dentate neurogenesis after brain injury undermines long-term neurogenic potential and promotes seizure susceptibility. Stem Cell Rep. 9, 972–984. https://doi.org/10.1016/j.stemcr.2017.07.015.

Ngwenya, L.B., Danzer, S.C., 2019. Impact of traumatic brain injury on neurogenesis. Front. Neurosci. 12, 1014. https://doi.org/10.3389/fnins.2018.01014.

Ngwenya, L.B., Mazumder, S., Porter, Z.R., Minnema, A., Oswald, D.J., Farhadi, H.F., 2018. Implantation of neuronal stem cells enhances object recognition without increasing neurogenesis after lateral fluid percussion injury in mice. Stem Cells Int. 2018, 1–11. https://doi.org/10.1155/2018/4209821.

Ngwenya, L.B., Peters, A., Rosene, D.L., 2005. Light and electron microscopic immunohistochemical detection of bromodeoxyuridine-labeled cells in the brain: different fixation and processing protocols. J. Histochem. Cytochem. 53, 821–832. https://doi.org/10.1369/jhc.4A6605.2005.

Noshita, N., Lewen, A., Sugawara, T., Chan, P.H., 2002. Akt phosphorylation and neuronal survival after traumatic brain injury in mice. Neurobiol. Dis. 9, 294–304. https://doi.org/10.1006/nbdi.2002.0482.

Osier, N.D., Carlson, S.W., DeSana, A., Dixon, C.E., 2015. Chronic histopathological and behavioral outcomes of experimental traumatic brain injury in adult male animals. J. Neurotrauma 32, 1861–1882. https://doi.org/10.1089/neu.2014.3680.

Pardo, M., Abrial, E., Jope, R.S., Beurel, E., 2016. GSK3beta isoform-selective regulation of depression, memory and hippocampal cell proliferation. Genes Brain Behav. 15, 348–355. https://doi.org/10.1111/gbb.12283.

Rola, R., Mizumatsu, S., Otsuka, S., Morhardt, D., Noblehaeusslein, L., Fishman, K., Potts, M., Fike, J., 2006. Alterations in hippocampal neurogenesis following traumatic brain injury in mice. Exp. Neurol. 202, 189–199. https://doi.org/10.1016/j.expneurol.2006.05.034.

Sahay, A., Scobie, K.N., Hill, A.S., O'Carroll, C.M., Kheirbek, M.A., Burghardt, N.S., Fenton, A.A., Dranovsky, A., Hen, R., 2011. Increasing adult hippocampal neurogenesis is sufficient to improve pattern separation. Nature 472, 466–470. https://doi.org/10.1038/nature09817.

Shapira, M., Licht, A., Milman, A., Pick, C.G., Shohami, E., Eldar-Finkelman, H., 2007. Role of glycogen synthase kinase-3beta in early depressive behavior induced by mild traumatic brain injury. Mol. Cell. Neurosci. 34, 571–577. https://doi.org/10.1016/j.mcn.2006.12.006.

Shapiro, L.A., 2017. Altered hippocampal neurogenesis during the first 7 days after a fluid percussion traumatic brain injury. Cell Transplant. 26, 1314–1318. https://doi.org/10.1177/0963689717714099.

Shim, S.S., Stutzmann, G.E., 2016. Inhibition of glycogen synthase kinase-3: an emerging target in the treatment of traumatic brain injury. J. Neurotrauma 33, 2065–2076. https://doi.org/10.1089/neu.2015.4177.

Sun, D., Colello, R.J., Daugherty, W.P., Kwon, T.H., McGinn, M.J., Harvey, H.B., Bullock, M.R., 2005. Cell proliferation and neuronal differentiation in the dentate gyrus in juvenile and adult rats following traumatic brain injury. J. Neurotrauma 22, 95–105. https://doi.org/10.1089/neu.2005.22.95.

Sun, D., Daniels, T.E., Rolfe, A., Waters, M., Hamm, R., 2015. Inhibition of injury-induced cell proliferation in the dentate gyrus of the hippocampus impairs spontaneous cognitive recovery after traumatic brain injury. J. Neurotrauma 32, 495–505. https://doi.org/10.1089/neu.2014.3545.

Taylor, C.A., Bell, J.M., Breiding, M.J., Xu, L., 2017. Traumatic brain injury–related emergency department visits, hospitalizations, and deaths — United States, 2007 and 2013. MMWR Surveill. Summ. 66, 1–16. https://doi.org/10.15585/mmwr.ss6609a1.

Thompson, H.J., Lifshitz, J., Marklund, N., Grady, M.S., Graham, D.I., Hovda, D.A., McIntosh, T.K., 2005. Lateral fluid percussion brain injury: a 15-year review and evaluation. J. Neurotrauma 22, 42–75. https://doi.org/10.1089/neu.2005.22.42.

Toth, Z., Hollrigel, G.S., Gorcs, T., Soltesz, I., 1997. Instantaneous perturbation of dentate interneuronal networks by a pressure wave-transient delivered to the neocortex. J. Neurosci. Off. J. Soc. Neurosci. 17, 8106–8117.

Van, K.C., Lyeth, B.G., 2016. Lateral (parasagittal) fluid percussion model of traumatic brain injury. Methods Mol. Biol. 1462, 231–251. https://doi.org/10.1007/978-1-4939-3816-2_14.

Villasana, L.E., Kim, K.N., Westbrook, G.L., Schnell, E., 2015. Functional integration of adult-born hippocampal neurons after traumatic brain injury. eNeuro 2. https://doi.org/10.1523/ENEURO.0056-15.2015.

Wang, Y., Sawyer, T.W., Tse, Y.C., Fan, C., Hennes, G., Barnes, J., Josey, T., Weiss, T., Nelson, P., Wong, T.P., 2017. Primary blast-induced changes in Akt and GSK3β phosphorylation in rat hippocampus. Front. Neurol. 8, 413. https://doi.org/10.3389/fneur.2017.00413.

Wu, X., Mao, H., Liu, J., Xu, J., Cao, J., Gu, X., Cui, G., 2013. Dynamic change of SGK expression and its role in neuron apoptosis after traumatic brain injury. Int. J. Clin. Exp. Pathol. 6, 1282–1293.

Zhao, S., Fu, J., Liu, X., Wang, T., Zhang, J., Zhao, Y., 2012. Activation of Akt/GSK-3beta/beta-catenin signaling pathway is involved in survival of neurons after traumatic brain injury in rats. Neurol. Res. 34, 400–407. https://doi.org/10.1179/1743132812Y.0000000025.